Lasers in Surgery and Medicine 23:194–203 (1998)

Optical Properties of Native and Coagulated Human Liver Tissue and Liver Metastases in the Near Infrared Range

Christoph-Thomas Germer, MD,[1]* André Roggan, PhD,[2] Joerg P. Ritz, MD,[1] Christoph Isbert, MD,[1] Dirk Albrecht, MD,[1] Gerhard Müller, PhD,[2] and Heinz J. Buhr, MD, FACS[1]

[1]Department of Visceral, Vascular and Thoracic Surgery, University Hospital Benjamin Franklin, Freie Universität Berlin, Berlin, Germany
[2]Institute of Medical Physics/Laser Medicine, University Hospital Benjamin Franklin, Freie Universität Berlin, Berlin, Germany

Background and Objective: **Knowledge about optical parameters and the resultant light distribution in laser-treated tissue is important for predicting the effects of laser-induced thermotherapy of liver metastases (LITT).**
Materials and Methods: **The absorption and scattering coefficients as well as the anisotropy factors and the optical penetration depths of human liver tissue and colorectal liver metastases were determined at 850, 980, and 1,064 nm under native and thermocoagulated conditions.**
Results: **Liver metastases had a lower anisotropy factor, absorption, and scattering coefficient than healthy liver ($P < 0.01$), resulting in a significantly higher optical penetration depth in metastatic tissue. Coagulation significantly changes the optical parameters by reducing the optical penetration depth in both tissue types ($P < 0.01$).**
Conclusions: **A greater optical penetration depth in metastatic tissue is advantageous for LITT, since larger tumor volumes can be coagulated. At the same time, an adjustment of the application parameters during LITT is necessary to achieve optimal therapeutic success. Lasers Surg. Med. 23:194–203, 1998.**

Key words: optical properties; dosimetry; laser-induced thermotherapy; liver metastases

INTRODUCTION

The liver is the most common manifestation site of distant metastases from colorectal carcinomas. In ~25% of the patients, liver metastases are concomitantly detected already at the time of primary diagnosis. Another 50% develop metachronous hepatic metastases, the liver frequently being the only site of metastasis [1,2]. However, only a maximum of 30% of patients can be considered for surgical resection, which is currently the only established standard procedure for the treatment of liver metastases [3]. For this reason, it is necessary to standardize other treatment concepts such as laser-induced thermotherapy (LITT), first described by Bown in 1983 [4]. Precise knowledge about the spatial distribution of induced thermal

Contract grant sponsor: Deutsche Forschungsgemeinschaft (DFG); Contract grant no.: A1 443/1-1.

*Correspondence to: Christoph-Thomas Germer, MD, Department of Visceral, Vascular and Thoracic Surgery, University Hospital Benjamin Franklin, Freie Universität Berlin, Hindenburgdamm 30, 12200 Berlin, Germany.
E-mail: Germer@ukbf.fu-berlin.de

Accepted 7 August 1998

tissue damage and the temperature distribution in the specific target organ as well as its dependency on the selected application parameters is of decisive importance for the safe application of laser-induced thermotherapy. Ideally, it should already be possible to plan the required application parameters in advance so that treatment can be precisely adjusted to the individual findings. The calculation of laser-induced thermal tissue reactions is a complex task in which the computation of laser light distribution in scattering and absorbing media is of primary importance [5,6]. This requires knowledge about the optical parameters (absorption, scattering, anisotropy) of the target tissue, which may considerably differ depending on the tissue structure. Especially in laser-induced thermotherapy of liver metastases, it is necessary to determine these parameters not only in the healthy liver but also in metastatic tissue. Thus the aim of this experimental study was to determine the optical parameters in human liver tissue as well as in colorectal liver metastases at wavelengths of 850, 980, and 1,064 nm usually used for LITT. Because changes in the optical parameters even occur during laser application due to thermocoagulation, they were examined in both the native and coagulated tissue state. In addition, the results were evaluated for interindividual differences that might be important for individual calculations. To confirm the precision of our experimental setup, optical parameters were also assessed for intraindividual sample differences by measuring three independent samples from each patient and tissue type.

MATERIALS AND METHODS

Acquisition and Preparation of Tissue Samples

We examined three liver and three metastatic tissue samples from 10 patients (6 males, 4 females), yielding a total of 60 tissue samples. All tumor samples were metastases from adenocarcinomas with various differentiation grades (1 well, 4 moderately, 5 slightly differentiated). All patients underwent partial liver resection in our surgical department. A tissue block was removed from the resection samples in the operating room immediately after surgery. Three samples from normal liver and metastatic tissue were taken from each patient. The samples were cut into cubes with a 5-mm edge length and frozen in liquid nitrogen (77K). The cubes were then homogenized in a precooled mortar. The homogenate was placed into cylindrical quartz cuvetts with a defined sample thickness of 200 μm (normal liver tissue) and 500 μm (liver metastases). According to comparative examinations by Peters et al., the optical parameters of cut and homogenized tissue samples deviate by a maximum of 3% [7]. The histological examinations after preparation revealed that the cell morphology was intact and the cell units remained in tissue clusters (50–200 μm in diameter) (Fig. 1).

After measuring the optical properties in the native tissue state, each sample was completely coagulated in a water bath at 80° C for 10 minutes to evaluate the effect of thermocoagulation (Fig. 2). The samples were not removed from the cuvets to prevent water contact or osmotic interaction. In this way, three independent samples from each patient and tissue type (normal liver/tumor) were prepared and measured in their native and coagulated states.

Experimental Setup

Macroscopic optical parameters, diffuse remission (R_d), total transmission (T_t), and collimated transmission (T_c) were measured at wavelengths of 850, 980, and 1,064 nm using a double integrating sphere system (Fig. 3). The tissue samples were placed between both integrating spheres (200 mm). The remitted and transmitted intensities were optically integrated by the highly reflective coating of the integrating spheres. The resultant homogenous power density on the inner surface of the spheres was recorded by photodetectors. Baffles in the spheres ensured that the detectors recorded only the multiply scattered beam components and not those directly emitted by the tissue samples. Collimated (nonscattered) transmission (T_c) was finally measured using an additionally installed sphere. A Mercury arc lamp (Osram HBO100W/2, 0.4 mm arc length, 2×10^6 cd/cm^2) was selected as light source. The distance from the light source to the target tissue was 1,000 mm. A grid monochromator in Czerny-Turner configuration with a stepper motor (AMKO, 01-002SF, 200 mm focal length) was used for wavelengths selection. The width of the monochromator slits was set to 1 mm for all measurements. The monochromator emergent ray was projected onto the tissue sample with a spherical mirror (100 mm, f = 250 mm). The beam path was set at an image ratio of 1:3 leading to an illumination area of 3 mm in diameter on the tissue sample. The reference intensity was

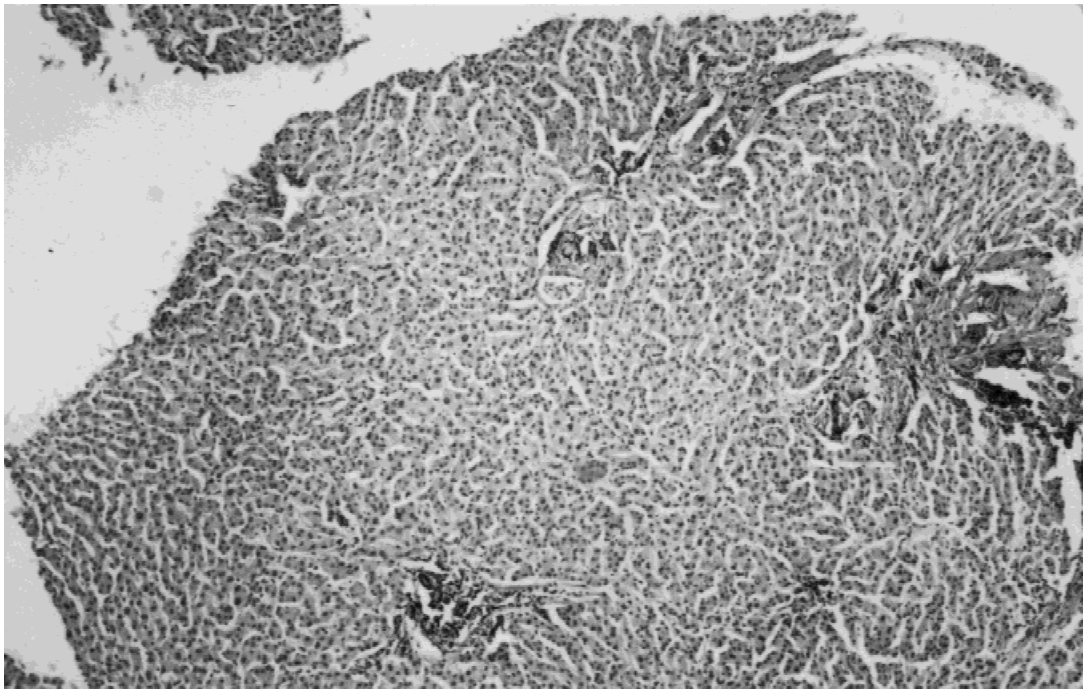

Fig. 1. Histological section of homogenized liver tissue showing tissue clusters with intact cells (5 μm, hematoxylin & eosin, 20×).

measured in a partial beam to eliminate intensity fluctuations. The partial beam was provided by a refelecting chopper wheel at a frequency of 220 Hz. Radiation fields in the integrating spheres were determined using silicon photodiodes and an integrated preamplifier (AMKO 09SiU04-C). A lock-in amplifier technique was applied (ITHACO 3981) to further process the measurement signals.

Evaluation

For evaluating measurements and calculating the optical parameters, inverse Monte Carlo simulation was applied to consider prescisely the geometric and optical conditions (sample geometry, sphere parameter, refractive index jumps, screen diameter, ray divergence, etc.) and thus compensate for all systematic errors [6,8]. To calculate the optical parameters with Monte Carlo simulations, an initial set of optical properties had to be estimated on the basis of the measurements obtained by an analytical model (Kubelka-Munk theory) [9]. A Monte Carlo simulation of the measurement parameters (R_d, T_t, T_c) was performed based on this initial set of data. In this way, all geometry-dependent systematic errors were compensated and the interaction of the radiation fields corrected, thus providing a simulated set of measurement data that could be compared to the actual measurements. If agreement between calculated and measured data was within a defined error limit, the set of optical parameters was accepted for the sample. Otherwise, three consecutive simulations were performed, in which one of the three parameters μa, μs, or g was slightly varied in each calculation. An improved set of optical parameters could then be determined from the final gradient matrix and deviations of the calculated measurement parameters. The variation calculation was repeated until the deviation between measurements and simulation were within (0.15%, Fig. 4). Optical penetration depth was calculated as previously described [6].

Statistics

The optical parameters are given as mean values with their standard error of the mean. First, the means for each patient were calculated from the three sample measurements of tissue type and state. This yielded information about measurement precision. Second, the means for all patients were calculated to obtain data on the interindividual variability of optical properties. The Wilcoxon U test for unpaired random samples

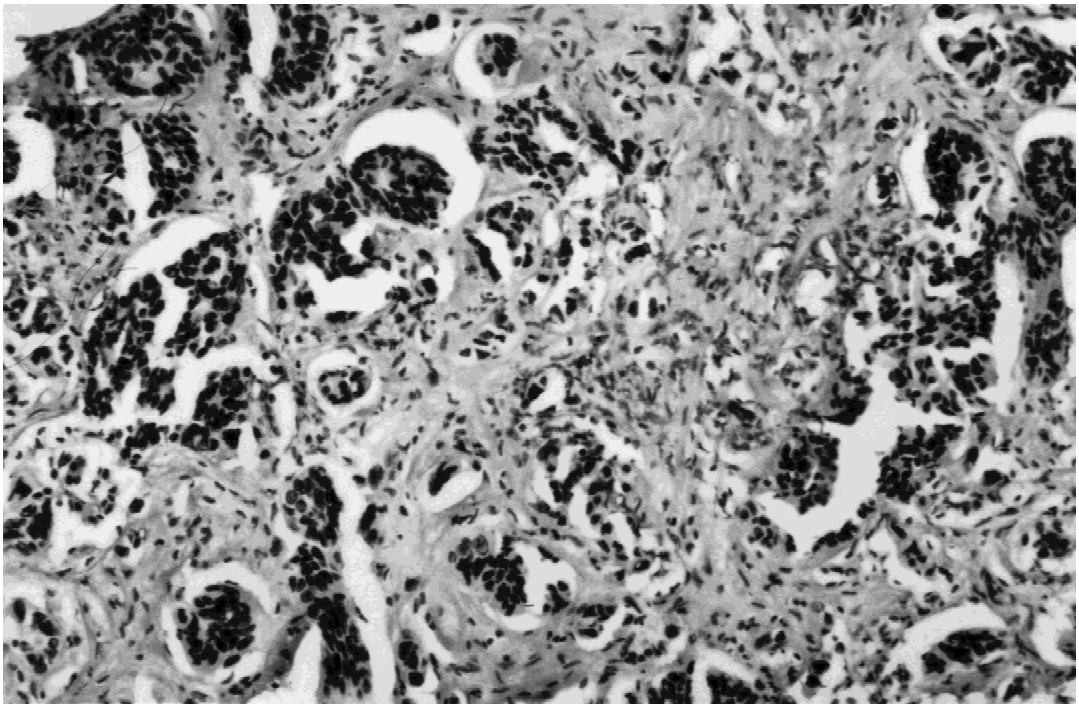

Fig. 2. Histological section of human colorectal liver metastases after thermocoagulation at temperature of 80°C (5 μm, hematoxylin & eosin, 50×).

was used for statistical analysis and the Friedman test for the comparison of more than two random samples. The level of significance was set at $P < 0.01$.

RESULTS

Wavelength

With an increasing wavelength from 850 to 1,064 nm in native tissue, there was a significant decrease in the absorption coefficient from 0.10 mm^{-1} to 0.05 mm^{-1} (liver) and from 0.06 mm^{-1} to 0.03 mm^{-1} (metastasis) (Table 1). The scattering coefficient showed a significant wavelength dependence only in normal liver tissue with a decrease from 20.4 mm^{-1} at 850 nm to 16.9 mm^{-1} at 1,064 nm. Comparing the optical penetration depth in both liver tissue and colorectal liver metastases at the three wavelengths revealed that the highest penetration depth was achieved at a wavelength of 1,064 nm (3.0 mm in liver, 4.2 mm in metastatses).

Tissue Type (Liver/Metastasis)

At all three wavelengths examined, there were significant differences between both tissue types in the native state (Table 1). The absorption coefficient of normal liver was always higher than in metastatic tissue (0.10 mm^{-1} vs. 0.06 mm^{-1} at 850 nm; 0.05 mm^{-1} vs.0.03 mm^{-1} at 1,064 nm). The scattering coefficient and the anisotropy factor of normal liver tissue were also significantly higher at all three wavelengths than in metastatic tissue. The resulting optical penetration depths were significantly higher in metastatic tissue at all three wavelengths (Fig. 5).

Thermocoagulation

Thermocoagulation of tissue led to significant changes in the optical parameters. In both liver and metastatic tissue, there was a decrease in the absorption coefficient, an increase in the scattering coefficient,and a decrease in the anisotropy factor after thermocoagulation. The optical penetration depth is reduced at all three wavelengths by 23% in normal liver and by 15% in metastatic tissue. The absolute values decreased by 0.5 mm (liver) and 0.4 mm (metastatic) at 850 nm, by 0.5 mm (liver and metastatic) at 980 nm and by 0.5 mm (liver) and 0.7 mm (metastatic) at 1,064 nm (Fig. 6). In the comparison of both tissue types after thermocoagulation, significantly higher values for the absorption and scattering coefficients as well as the anisotropy factor still

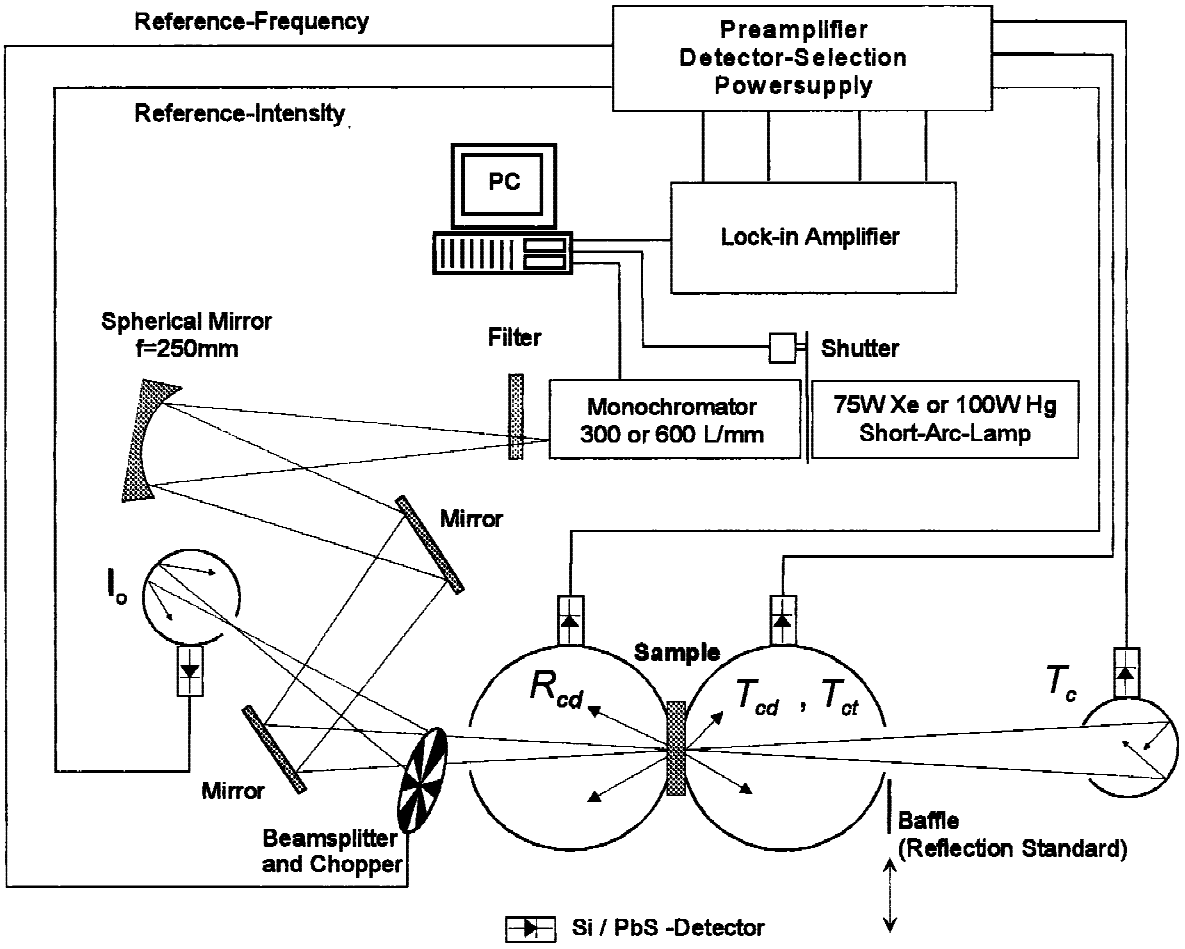

Fig. 3. Illustration of experimental set-up for the measurement of optical tissue properties (R_d: diffuse reflexion, T_d: diffuse transmission, T_c: collimated transmission).

occurred in normal liver tissue at all three wavelengths, while differences in the absorption behavior were not significant (Table 2). There was an optical penetration depth of 1.3 mm (850 nm), 1.7 mm (980nm) and 2.5 mm (1,064 nm) for coagulated liver tissue compared to 1.9 mm, 2.7 mm and 3.6 mm in the tissue of colorectal liver metastases.

Intraindividual and interindividual variance. In the comparison of the three samples of one patient corresponding to the intraindividual standard deviation, the optical parameters did not significantly differ in either the healthy or the metastatic liver tissue. In contrast, there were significant differences in the intraindividual standard deviation between both tissue types (normal liver/metastases). Comparing the interindividual standard deviation revealed significant differences between various patients. In general, variations in tumor tissue were clearly higher than those in liver tissue. The mean standard deviation of the absorption coefficient varied between 18% (liver) and 30.6% (metastases) for all three wavelengths and both tissue states (native/coagulated). The values for the scattering coefficient and anisotropy factor were 17% and 1.2% in healthy tissue and 19.2% and 2.9% for colorectal liver metastases. Interindividual standard deviation for the optical penetration depth was 14.4% (liver) and 23.1% (metastases).

DISCUSSION

In contrast to laser application for surgical resection of intrahepatic tumors, where the effect is directly visible, the result of LITT usually escapes direct visual control due to the selected access or the anatomic location of the target region [10]. Thus, the resulting lesion can only be visualized indirectly via imaging procedures such as

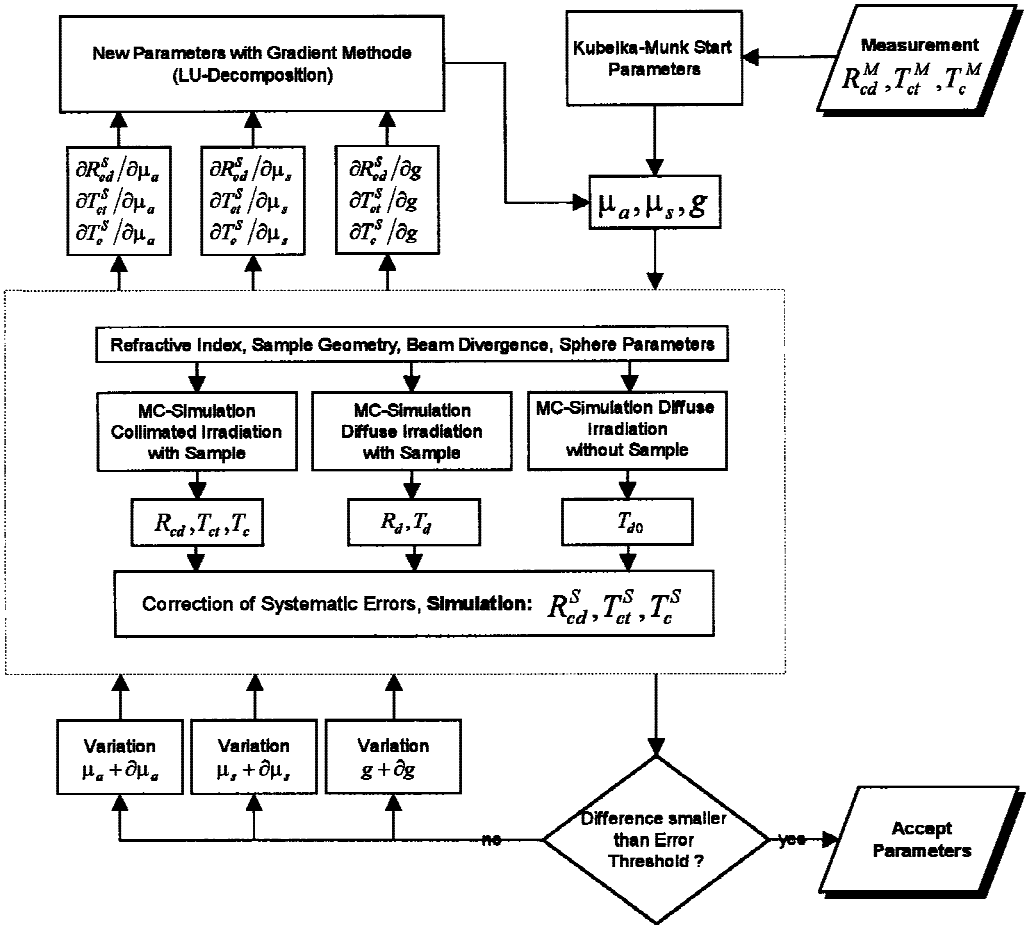

Fig. 4. Flowchart of the inverse Monte Carlo simulation.

TABLE 1. Optical Properties of Normal and Metastatic Human Liver Tissue *Before* Thermal Coagulation (Mean ± SEM), n = 10

	Normal liver tissue			Liver metastases		
Wavelength (nm)	850	980	1,064	850	980	1,064
Absorption coefficient (mm^{-1})	0.10 ± 0.02	0.08 ± 0.01	0.05 ± 0.01	0.06 ± 0.02	0.06 ± 0.02	0.03 ± 0.01
Scattering coefficient (mm^{-1})	20.4 ± 3.6	18.2 ± 3.3	16.9 ± 3.3	10.8 ± 1.1	11.3 ± 1.6	10.9 ± 1.9
Anisotropy	0.955 ± 0.01	0.955 ± 0.01	0.952 ± 0.01	0.902 ± 0.02	0.914 ± 0.02	0.917 ± 0.02
Optical penetration depth (mm)	1.8 ± 0.27	2.2 ± 0.3	3.0 ± 0.4	2.3 ± 0.5	2.7 ± 0.6	4.2 ± 0.9

TABLE 2. Optical Properties of Normal and Metastatic Human Liver Tissue *After* Thermal Coagulation (Mean ± SEM), n = 10

	Normal liver tissue			Liver metastases		
Wavelength (nm)	850	980	1,064	850	980	1,064
Absorption coefficient (mm^{-1})	0.07 ± 0.02	0.05 ± 0.01	0.02 ± 0.01	0.05 ± 0.02	0.05 ± 0.01	0.02 ± 0.01
Scattering coefficient (mm^{-1})	23.6 ± 4.7	21.0 ± 2.7	20.0 ± 2.68	10.4 ± 2.0	10.5 ± 2.17	10.3 ± 2.1
Anisotropy	0.887 ± 0.02	0.896 ± 0.02	0.904 ± 0.01	0.827 ± 0.04	0.860 ± 0.02	0.865 ± 0.02
Optical penetration depth (mm)	1.3 ± 0.2	1.7 ± 0.3	2.5 ± 0.4	1.9 ± 0.5	2.2 ± 0.43	3.5 ± 0.9

ultrasound or magnetic resonance imaging. Even if both procedures basically appear suitable as so-called on-line techniques for demonstrating morphological changes during interstitial laser application [11,12], it is impossible to precisely visualize an exact temperature course or the course of a thermal damage zone under in vivo conditions [13,14,15]. Moreover, thermal tissue reactions in

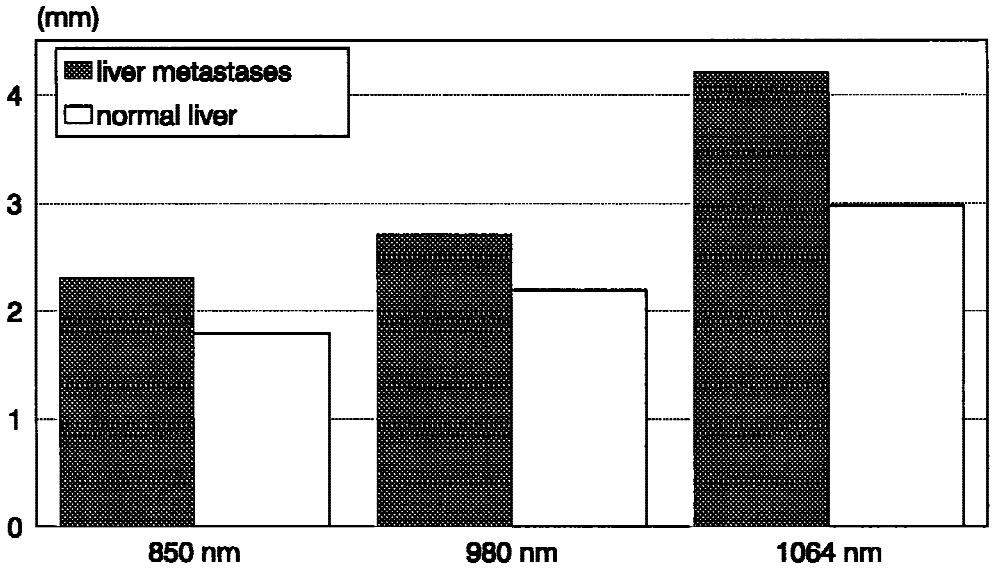

Fig. 5. Optical penetration depth (mm) of normal and metastatic liver tissue *before* thermal coagulation at three wavelengths (* = $P < 0.05$ normal tissue in relation the the metastatic tissue).

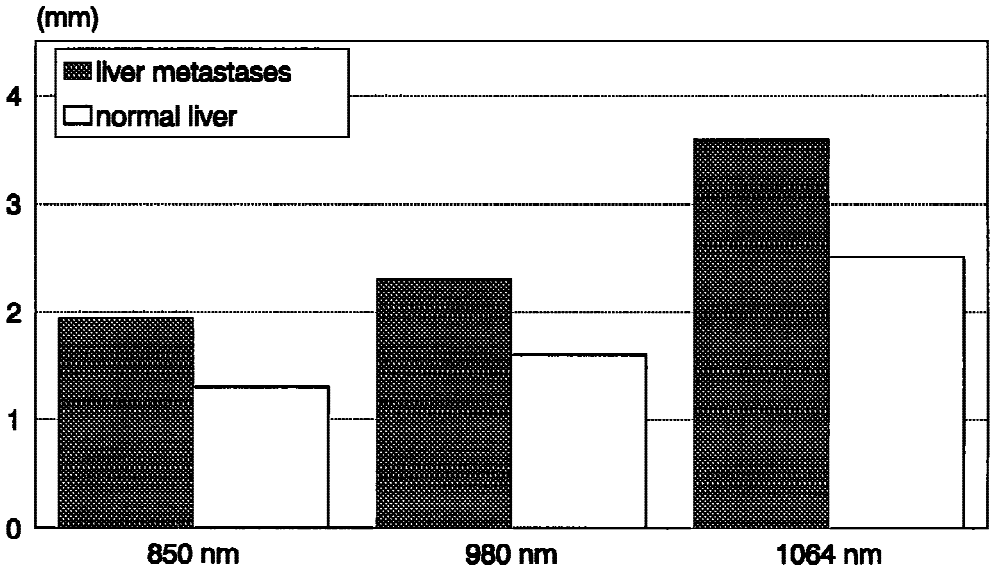

Fig. 6. Optical penetration depth (mm) of normal and metastatic liver tissue *after* thermal coagulation at three wavelengths (* = $P < 0.05$ normal tissue in relation to the metastatic tissue).

a temperature range of 45° to 60° C such as those induced in the marginal region of interstitial laser application are not immediately detectable morphologically but only become manifest after a delay of several days or weeks [16,17].

Since the local temperature in the treated tissue and thus the size of the thermal damage zone are directly influenced by light diffusion, knowledge of the optical parameters is of decisive importance for the clinical application of LITT for the treatment of malignant liver tumors [18,19]. Despite this importance, few studies have thus far determined these parameters for human liver tissue and for metastatic tissue at the wavelengths relevant for laser-induced thermotherapy. The study performed by Marchesini et al. recorded optical parameters of human liver tissue only at wavelengths of 514 and 633 nm [20]. Nakamura et al. [21] determined the optical penetration depth of healthy human liver and liver metastasis only at wavelengths of 410, 630 and 670 nm. Otherwise comparability of results from

animal tissue with the optical parameters of human liver tissue appears to be problematic. Our previous studies have revealed up to 300% differences in the optical parameters of human and porcine liver tissue [6]. Moreover, knowledge of the optical parameters only in the native untreated tissue state is inadequate for optimized clinical application, since thermal tissue denaturation leads to microscopic changes in the cellular and protein structures that imply similar changes in the optical parameters [22–26]. However, the literature still lacks data on the thermally induced changes in the optical parameters of human liver tissue or tissue of colorectal liver metastases. Therefore, the aim of the present study was to determine the optical parameters of human liver tissue and tissue of colorectal liver metastases at the LITT-relevant wavelengths of 850, 980 and 1,064 nm and to examine the impact of thermal coagulation on these parameters.

The optical tissue parameters were determined in vitro using a double integrating sphere system. This indirect measuring method applies approaches in solving the radiation transport equation which make it possible to consider multiple scattering and directional changes of the incident ray. This enables the measurement of tissue samples with a thickness of up to several hundred micrometers. The double integrating sphere system can be regarded as the measuring procedure with the highest precision for determining the complete set of optical properties with only one experimental set-up [6,27–31]. It has already been used to perform numerous investigations for determining the optical parameters of human and animal tissues like aorta, prostate, brain, bladder, myocardium, colon, esophagus, skin and blood [7,18,20,23,27]. Inverse Monte Carlo simulation was the evaluation procedure with the highest precision. This stochastic procedure was developed for the simulation of physical processes. It was first applied in 1984 by Wilson [32] to examine radiation transport processes in biological tissue and has since been taken up by various authors [33–35]. The advantage of Monte Carlo simulation is that it enables precise consideration of the geometric and optical conditions (sample geometry, sphere parameters, refractive index, beam divergence, etc.). Agreement between Monte Carlo calculations and the actual conditions has been verified in a series of studies on models with defined optical parameters [32,36].

When relating the optical tissue parameters to the selected wavelengths (850–1,064 nm), their increase is associated with a decreased absorption coefficient with only a slightly altered scattering coefficient and anisotropy factor in both liver and metastatic tissue. The penetration depth increased and reached a maximum in the wavelength range of the Nd:YAG laser at 3.0 mm in the normal liver and 4.2 mm in metastatic tissue. In analogy to these results, Parsa et al. [37], examining this wavelength for rat liver, also found a minimum absorption and a maximum penetration depth of 7.1 mm. From a clinical point of view, the optical penetration depth of the laser light in the target tissue should be as high as possible to keep the temperature gradients between the laser applicator and the periphery of the laser-induced lesion as flat as possible. This reduces the danger of overheating and prevents carbonization and vaporization of the tissue.

If the results are differentiated in relation to the tissue type, we found that in normal liver tissue the absorption coefficient is 60% and the scattering coefficient 70% higher than in metastatic tissue. Similarly, the anisotropy factor was 0.04 higher in healthy tissue. Consequently, the optical penetration depth was about 33% higher in tumor tissue at all three examined wavelengths. Comparing the optical parameters of healthy and tumorous liver tissue in rats, Van Hillegersberg et al. [31] also reported increased absorption, scattering and anisotropy in healthy tissue, and a 60% increase in the penetration depth of tumor tissue. In a comparison of healthy and tumorous breast tissue, Peters et al. [7] found the same differences at a wavelength of 900 nm. He described a 25% higher penetration depth for breast carcinoma tissue. Determining the optical penetration depth of healthy and metastatic human liver at the wavelengths of 410, 630 and 670 nm, Nakamura et al. [21] likewise found a significantly higher penetration depth in tumor tissue. From a clinical point of view, these facts represent a considerable advantage in the treatment of liver metastases, since a greater tumor volume can be treated with the optimal adjustment of laser power. A possible explanation for this result is the significantly lower content of hemoglobin, mitochondrial cytochromoxidase, mitochrocytes and DNA in tumor tissue, since they strongly effect the optical tissue parameters [38].

When considering the effect of thermocoagulation, we found a considerable impact on the optical parameters, which was more pronounced in normal liver than in tumor tissue. In both tissue

types, change in scattering behavior with a decrease in the anisotropy factor and an increase in the scattering coefficient led to a 23% reduction of the optical penetration depth in normal liver and a 20% reduction in metastatic tissue. Pickering et al. [39] obtained similar results on coagulated healthy rat liver. Splinter et al. [30] showed that the optical parameters of myocardial tissue also changed and resulted in a reduction of the penetration depth from 3.9 to 2.9 mm (26 %). A possible reason for this is the alteration of the protein tertiary structure due to the destruction of absorbing chromophores such as hemoglobin or mitochondrial cytochromoxidase and the thermally induced break-down of disulfide bonds as described by Mirza et al. [40]. Differences between healthy and tumor tissue may be explained by a greater content of necrosis in the tumor samples examined. The necrotic component would only be subject to a slight change due to thermocoagulation. In addition, the reduced amount of chromophores and scattering components in tumors influences the behavior of the optical parameters during thermocoagulation. The clinical consequence of these findings is the demand that the application parameters should not be kept constant for the entire LITT of liver metastases. They have to be continuously or gradually adjusted *during* therapy in order to achieve optimal adaptation to the actual optical penetration depth throughout the application and thus reach the maximum treatable lesion volume. Comparing our sample results from one patient (intraindividual standard deviation), no significantly differing optical parameters were found in either liver or metastatic tissue. This is an expression of the high precision of the chosen experimental set-up. When considering the interindividual variance of normal liver tissue, it was significantly lower for all measurements than that of metastatic tissue. Tumor tissue showed higher patient-dependent variations than normal liver tissue of up to 70% for the absorption coefficients, 20% for the scattering coefficients, 140% for the anisotropy factor and 60% for the optical penetration depth. The study by Van Hillegersberg et al. [31] describes an up to 100% higher standard deviation in the optical properties of tumor tissue than in those of healthy tissue in rats. This means that the tumor samples from various individuals vary more strongly in their optical parameters than the healthy tissue samples from these persons. These results reflect the more inhomogeneous phenotype of metastatic tissue compared to normal liver. However the degree of differentiation in the present study exerted no significant influence on the optical parameters. The results clearly show how problematic it is to apply the optical tissue parameters measured in healthy liver to those in tumor tissue.

CONCLUSION

With regard to the optical parameters, there are considerable differences between healthy human liver tissue and tissue of colorectal liver metastases. Tumor tissue has a lower absorption and scattering coefficient as well as anisotropy factor than healthy tissue, subsequently resulting in a higher optical penetration depth of the laser light into metastatic tissue. This is advantageous in the therapy of liver metastases, since a greater tumor volume can be treated by optimal laser power adjustment.

Thermal tissue coagulation leads to considerable changes in the optical parameters during LITT. After coagulation, the absorption coefficient and anisotropy factor decrease, while the scattering coefficient increases (except in tumor tissue). Thus, there is the demand that the application parameters should not be kept constant for the entire LITT application of liver metastases. They should be continuously or gradually adapted *during* therapy in order to achieve the maximum treatable lesion volume.

Optical parameters are subject to significant patient-related deviations (interindividual differences), which particularly occur in metastatic tissue. With regard to therapy optimization, further studies are necessary to clarify the effects of histological grading, tumor volume and necrosis on optical parameters

REFERENCES

1. Pickren JW, Tsukuda Y, Lane WW. Liver metastases: Analysis of autopsy data. In: Weiss L, Gilber HA, eds. "Liver metastases." Boston: GK Hall, 1984: 2–18.
2. Taylor I. Liver metastases from colorectal cancer: Lessons from past and present studies. Br J Surg 1996; 83:456–460.
3. Scheele J, Stangl R, Altendorf-Hofmann A, Paul M. Resection of colorectal metastases. World J Surg 1995; 19:59–71.
4. Bown SG. Phototherapy of tumors. World J Surg 1983; 7:700–709.
5. Roggan A, Müller G. Dosimetry and computer based irradiation planning for laser-induces interstital thermotherapy (LITT). In: Müller G, Roggan A, eds. "Laser-induced Interstitial Thermotherapy." Bellingham, WA: SPIE Press, 1995: 114–157.

6. Roggan A. Dosimetrie thermischer Laseranwendungen in der Medizin-Untersuchung der optischen Gewebeeigenschaften und physikalisch-mathematische Modellentwicklung. Dissertation 1997; Fachbereich Physik, Technische Universität, Berlin.
7. Peters VG, Wyman DR, Patterson MS, Frank GL. Optical properties of normal and diseased human breast tissues in the visible and near infrared. Phys Med Biol 1990; 35: 1317–1334.
8. Roggan A, Minet O, Schröder C, Müller G. Measurements of optical properties of tissue using integrating sphere technique. In: Müller G, et al., eds. "Medical Optical Tomography: Functional Imaging and Monitoring." Bellingham, WA: SPIE Press, 1993; 149–165.
9. Kubelka P, Munk F. Ein Beitrag zur Optik der Farbanstriche. Z Techn Phys 1931; 12:593–601.
10. Ravikumar TS. Interstitial therapies for liver tumors. Surg Oncol Clin North Am 1996; 2:365–377.
11. Vogl TJ, Müller PK, Hammerstingl R, Weinhold N, Mack MG, Philipp C, Deimling M, Beuthan J, Pegios W, Riess H, Lemmens HP, Felix R. Malignant liver tumors treated with MR imaging-guided laser-induced thermotherapy: Technique and prospektive results. Radiology 1995; 196: 257–265.
12. Germer CT, Albrecht D, Roggan A, Isbert C, Buhr HJ. An experimental study of laparoscopic laser-induced thermotherapy treatment for liver tumours. Br J Surg 1997; 84: 317–320.
13. Dachman AH, McGehee JA, Beam TE, Burris JA, Powell DA. US-guided percutaneous laser ablation of liver tissues in a chronic pig model. Radiology 1990; 176:129–133.
14. Bosman S, Phoa SSK, Bosma A, Van Germert MJC. Effect of percutaneous interstitial thermal laser on normal liver of pig: sonographic and histopathological correlations. Br J Surg 1991; 78:572–575.
15. Anzai Y, Lufkin RB, Hirschowitz S, Farahani K, Castro DJ. MR imaging–Correlation of thermal injuries induced with intestitial Nd: YAG laser irradiation in the chronic model. J Magnet Res Imaging 1992; 2:671–678.
16. Thomsen S. Pathologic analysis of photothermal and photomechanical effects of laser-tissue interactions. Photochem Photobiol 1991; 53:825–835.
17. Johnson DE, Price RE, Cromeens DM. Pathological changes occuring in the prostate following transurethral laser prostatectomy. Lasers Surg Med 1992; 12:254–263.
18. Jacques SL. Laser-tissue interactions; photochemical, photothermal and photomechanical. Surg Clin N Am 1992; 72:531–558.
19. Gottschalk W, Hengst J. Influence of the laser-induced temperature rise in photodynamictherapy (PDT). Proceedings SPIE. Laser-Tissue-Interaction II, 1991; 1427: 320–326.
20. Marchesini R, Bertoni A, Andreola S, Melloni E, Sichirollo A. Extinction and absorption coefficients and scattering phase functions of human tissues in vitro. Appl Opt 1989; 28:2318–2324.
21. Nakamura S, Niskiwaki Y, Suzuki S, Sakaguchi S, Yamashita Y, Ohta K. Light attenuation of human liver and hepatic tumors after surgical resection. Lasers Surg Med 1990; 10:12–15.
22. Bosman S. Heat-induced structural alterations in myocardium in relation to changing optical properties. Appl Opt 1993; 32:461–463.
23. Derbyshire GJ, Bogen DK, Unger M. Thermally induced optical property changes in myocardium at 1.06 μm. Lasers Surg Med 1990; 10:28–34.
24. Jerath MR, Gardner CM, Rylander HG, Welch AJ. Dynamic optical property changes: Implications for reflectance feedback control of photocoagulation. Photochem Photobiol 1993; 16:113–126.
25. Thomsen S, Jacques SL, Flock S. Microscopic correlates of macroscopic optical property changes during thermal coagulation of myocardium. Proceedings SPIE 1992; 1202:2–10.
26. Welch AJ. The thermal response of laser irradiated tissue. IEEE J Quant Electron 1984; 20:1471–1481.
27. Cheong WF, Prahl SA, Welch AJ. A review of the optical properties of biological tissues. IEEE J Quant Electron 1990; 26:2166–2185.
28. Pickering JW, Prahl SA, Van Wieringen N, Beek JF, Sterenborg HJCM, Van Gemert MJC. Double-integrating sphere system for measuring the optical properties of tissue. Appl Opt 1993; 32:399–412.
29. Rastegar S, Jacques SL, Motomedi M, Kim BM. Theoretical analysis of equivalency of high-power diode laser (810 nm) and Nd: YAG Laser (1064 nm) for coagulation of tissues: predictions for prostate coagulation. Proceedings SPIE 1992; 1646:77–84.
30. Splinter R, Svenson RH, Littman L, Tuntelder JR, Chuang CH, Tatsis GP, Thompson M. Optical properties of normal, diseased and laser photocoagulated myocardium at the Nd: YAG wavelength. Lasers Surg Med 1991; 11:117–124.
31. Van Hillegersberg R, Pickering JW, Aalders M, Beek JF. Optical properties of rat liver and tumor at 633 nm and 1064 nm: photofrin enhances scattering. Lasers Surg Med 1992; 13:31–39.
32. Wilson BC, Adam G. A Monte Carlo model for the absorption and flux distributions of light in tissue. Med Phys 1984; 10:824–830.
33. Hourdakis CJ, Perris A. A Monte Carlo estimation of tissue optical properties for use in laser dosimetry. Phys Med Biol 1995; 40:351–364.
34. Key H, Davies ER, Jackson PC, Wells PNT. Monte Carlo modelling of light propagation in breast tissue. Phys Med Biol 1991; 36:591–602.
35. Kienle A, Steiner R. Determination of the optical properties of tissue by spatially resolved transmission measurements and Monte Carlo calculations. Proceedings SPIE 1994; 2077:142–152.
36. Flock ST, Wilson BC, Patterson MS. Monte Carlo modeling of light propagation in highly scattering tissues: comparison with measurements in phantoms. IEEE Trans Biomed Eng 1989; 36:1169–1173.
37. Parsa P, Jacques SL, Nishioka NS. Optical properties of rat liver between 350 and 2200 nm. Appl Opt 1989; 28:2325–2330.
38. Beauvoit B, Kitai T, Chance B. Contribution of the mitochondrial compartment to the optical properties of the rat liver: A theoretical and practical approach. Biophys J 1994; 67:2501–2510.
39. Pickering JW, Posthumus P, Van Gemert MJC. Continuous measurement of the heat-induced changes in the optical properties (at 1064 nm) of rat liver. Lasers Surg Med 1994; 15:200–205.
40. Mirza UA, Cohen SL, Chait B. Heat-induced conformational changes in proteins studied by electrospray ionization mass spectrometry. Anal Chem 1993; 65:1–6.